

RESEARCH

Open Access



An investigation into the biomechanical effects of tibial vertical cutting errors on the proximal tibia after unicompartmental knee arthroplasty and the improvement of cutting planes

Deyan Ou^{1†}, Gaoyong Deng^{2†}, Gaosheng Qin^{3†}, Yongqing Ye⁴, Jingwei Pan⁵, Yu Huang⁵, Haisheng Kuang¹, Shilin Tang⁵, Yongxin Mo⁵ and Shixin Pan^{5*}

Abstract

Objective Unicompartmental knee arthroplasty (UKA) has shown significant clinical effectiveness in treating medial compartment knee degeneration, but postoperative periprosthetic fractures and persistent pain remain common and challenging complications. Tibial vertical cutting errors are considered an important factor influencing postoperative biomechanics. This study aims to investigate the biomechanical effects of tibial vertical cutting errors (referring to the deviation between the actual vertical cutting plane and the ideal vertical resection plane during UKA) on the proximal tibia after UKA and to reduce the risk of fractures and improve postoperative outcomes through surface modification designs (chamfering and filleting).

Methods In this study, a three-dimensional model of the tibia was constructed from CT and MRI data of a 26-year-old male volunteer. Finite element analysis (FEA) was used to simulate different vertical cutting errors (1 mm, 3 mm, 5 mm, 7 mm, and 9 mm). The study included models with varying cutting errors and two surface modification designs. During the simulation, stress and strain distribution on the proximal tibia were analyzed to assess the impact of cutting errors on the risk of periprosthetic fractures. Additionally, the fracture risk was quantified using the Risk of Fracture (ROF) index, and statistical data analysis and comparison were performed.

Results The results showed that as the vertical cutting error increased, the equivalent stress and fracture risk value beneath the tibial prosthesis significantly increased. Notably, in the 5–9 mm cutting error models, the fracture risk was markedly higher. The chamfering and rounding designs effectively reduced stress concentration beneath the tibial prosthesis, lowering the stress peaks and significantly decreasing the fracture risk. In the ROF calculation, when the

[†]Deyan Ou, Gaoyong Deng and Gaosheng Qin contributed equally to this work.

*Correspondence:
Shixin Pan
honghuixmf@outlook.com

Full list of author information is available at the end of the article



vertical cutting error exceeded 5 mm, the ROF value significantly exceeded the critical value, indicating a substantial increase in fracture risk. Compared to the standard osteotomy method, both surface modification designs effectively reduced the fracture risk.

Conclusion Tibial vertical cutting error is a significant risk factor for periprosthetic fractures and pain after UKA. The greater the vertical cutting error, the faster the fracture risk and bone degeneration progress. Specifically, when the vertical cutting error exceeds 5 mm, the fracture risk increases significantly. The surface modification design proposed in this study effectively mitigates the negative biomechanical effects of cutting errors on the tibia and reduces the risk of postoperative complications. Future research should further explore the impact of other factors, such as osteoporosis, activity level, and muscle strength, on UKA outcomes, and incorporate advanced surgical navigation technologies to improve surgical precision and reduce errors.

Keywords UKA, Vertical cutting error, Surface modification, ROF

Introduction

UKA has become a common method for treating medial compartment knee degeneration. Its excellent clinical outcomes and well-established surgical procedures have gained increasing popularity among orthopedic surgeons [1, 2]. However, postoperative complications such as periprosthetic tibial fractures and persistent proximal tibial pain after UKA are severe complications that pose a significant trauma to the knee joint and present considerable challenges in treatment and management [3]. Currently, most clinical cases of periprosthetic fractures occur either intraoperatively or within the first few weeks postoperatively. The main causes include improper surgical techniques, early postoperative weight-bearing, osteoporosis, or reduced bone density [4, 5]. Due to the increasing number of UKA procedures performed annually, longer life expectancy, the rise in osteoporosis cases, and increased patient activity, the absolute number of patients facing fracture risk and persistent knee pain is on the rise [3, 6, 7]. Studies have shown that high stress and strain on cortical bone can impair bone remodeling, leading to bone degeneration [8, 9]. This abnormally high bone strain may be related to the geometry of the resection angle on the cutting surface. In UKA standard procedures, the current surgical technique involves using an extramedullary cutting guide to create orthogonal resection surfaces through vertical and horizontal cuts. This requires orthopedic surgeons to make precise cuts at right angles by hand with a bone saw, without the assistance of surgical robots, external navigation, or limiters. However, vertical cutting errors are common, especially when the resection is performed by inexperienced surgeons [10]. Current studies on tibial osteotomy have explored various aspects. Houskamp investigated the relationship between the depth of medial tibial plateau resection and the average maximum failure load, concluding that a resection depth exceeding 5.82 mm results in a significantly lower average failure load [11]. Stoddart, through the establishment of a finite element model, studied the risk of tibial eminence avulsion in

bicompartmental knee arthroplasty [12]. Dai, by establishing finite element models with varying tibial component angulations, studied the factors influencing stress distribution on the proximal tibia after UKA [13]. However, there is currently no clear research on the biomechanical effects of different extended vertical cuts on the tibia. In this study, we hypothesize that tibial vertical cutting errors affect the strain on the proximal tibia, and modifications to the surgical technique can prevent such extended vertical cutting errors. Furthermore, we established different geometries of resection angles on the cutting surface and analyzed, through finite element modeling, the impact of resection surface geometry on the interaction between the proximal tibia and the prosthesis.

Methods

Construction of the tibial 3D model

A healthy 26-year-old male volunteer (weight 70 kg, height 170 cm) was selected for the study. CT and MRI scans of the knee joint were performed, and model construction was carried out using the CT and MRI data. After scanning, the raw data from the machine were exported in DICOM format. To obtain a complete tibial structure, the data were imported into the Mimics 22.0 software (Materialise NV, Leuven, Belgium) for model preprocessing. Combining human anatomical data of the knee joint, the tibial structure was delineated in the software to create a complete tibial model. The generated tibial model was then imported into the medical reverse engineering software Geomagic Wrap 2021.0 (3D Systems, America), following the principle of maintaining the original physiological structure. After processing, the final NURBS surface was generated, and the STP format file was exported. This file was then imported into the finite element preprocessing software HyperWorks 21.0 (Altair, USA) for mesh generation and contact setting. The mesh diameter was set to 1.0 mm, and to better simulate the biomechanics of the tibia, the cortical and cancellous bones of the tibia were assigned common nodes.

Establishment of the tibial prosthesis finite element model and material assignment

The tibial dimensions were measured, and the tibial model was processed according to the standard tibial osteotomy procedure for a medial unicompartmental knee prosthesis with a fixed platform. A suitable tibial prosthesis was then selected [1, 14]. The mainstream Oxford medial fixed-platform unicompartmental knee prosthesis was selected for 3D modeling. The model includes the tibial prosthesis and polyethylene insert. After scanning the prosthesis using a 3D scanner, the data were imported into Geomagic Wrap 2021. Using the reverse engineering function, a 3D model of both the polyethylene insert and tibial prosthesis was generated. The tibial prosthesis was then moved upward by 1 mm to create a gap for filling with bone cement. The complete tibial and tibial prosthesis model was saved in STL format and imported into HyperWorks 21.0 for mesh generation. Using its mesh function, contact definitions and common node assignments were established. The finite element model of the tibia and tibial prosthesis was then completed and exported in INP format for further analysis. Referring to previous finite element studies on knee biomechanics, material properties were assigned to the tibial cortical bone, cancellous bone, tibial prosthesis, insert, and bone cement. The elastic modulus and Poisson's ratio for each structure were validated through existing literature [15–17]. (Table 1)

Establishment of the tibial extended vertical cutting model and surface modification model

Based on the tibial and tibial prosthesis models, a vertical cutting surface was simulated using a reciprocating saw with a width of 0.9 mm. Vertical cutting errors were set at 1 mm, 3 mm, 5 mm, 7 mm, and 9 mm, and corresponding models were created. Following the finite element modeling method for the tibial and tibial prosthesis models, different tibial extended vertical cutting models were established for analysis. For the surface modification models, two approaches were used: Chamfering: A chamfer was applied at the intersection of the vertical and horizontal planes, where the chamfer profile was an isosceles right triangle. The length of the right-angle sides was set to 1 mm, 2 mm, 3 mm, 4 mm, and 5 mm. Filletting: A fillet was applied at the intersection of the vertical

and horizontal planes, with different radii set at 1 mm, 2 mm, 3 mm, 4 mm, and 5 mm. Once the models were established, mechanical analysis was performed by applying a 1000 N load to the knee joint based on the load distribution between the medial and lateral compartments of the knee and the gait cycle. This load was used to simulate the forces acting on the knee joint during typical motion [18, 19]. (Fig. 1)

Calculation of fracture risk around the tibial prosthesis and statistical data analysis

Data collection primarily included the elastic limit strain and maximum principal strain beneath the tibial prosthesis. To calculate the fracture risk around the tibial prosthesis, the ROF standard was used. ROF refers to the maximum principal strain (ϵ) in the bone divided by the elastic limit strain value. In this study, under compressive load conditions, a higher ROF value in localized regions indicates a higher fracture risk. The formula for calculating ROF is as follows: $ROF = \epsilon / 0.0073$ if tensile and $\epsilon / 0.0104$ if compressive [12, 20]. Regions of interest (ROIs) Setting: To quantitatively assess the maximum principal strain and elastic limit strain, four ROIs were defined on the medial proximal tibia. ROI 1 was located at the innermost part of the proximal tibia, while ROIs 2 to 4 were progressively offset outward by 10 mm intervals, with ROI 4 situated slightly outside the center of the knee joint. These regions were selected as ROI because they represent common fracture sites, especially in cases with significant vertical cutting errors. This approach allows us to analyze the stress distribution on the tibial surface under different conditions and its impact on fracture risk. For each model, the von Mises stress and maximum principal strain at the nodes of ROIs 1 to 4 were collected, ROF was calculated, and the results were compared with the statistical values of the standard UKA osteotomy method. Statistical data processing was performed using IBM SPSS (x64 for Windows, version 22.0). Continuous data were expressed as $\bar{x} \pm s$. For data that followed a normal distribution, a one-sample t-test was used; for non-normally distributed data, a one-sample rank sum test was applied. A p -value of < 0.05 was considered statistically significant.

Knee joint model validation

To validate whether the established model can be used for further research, this finite element model was primarily validated using two methods based on previous studies: Method 1: The finite element model, subjected to the same loading conditions, was compared by identifying the high-risk fracture locations beneath the tibial prosthesis and comparing them with typical clinical fracture sites under tibial prostheses [3](Pandit et al., 2007). Method 2: The maximum ROF in the areas surrounding

Table 1 Material parameters of the tibia and unicompartmental prosthesis

Items	Young's modulus	Poisson's
Cortical bone	17,000	0.3
Methacrylate	1940	0.4
Polyethylene (PE)	850	0.4
Cancellous bone	350	0.25
Cobalt-chromiummolybde-num alloy	210,000	0.29

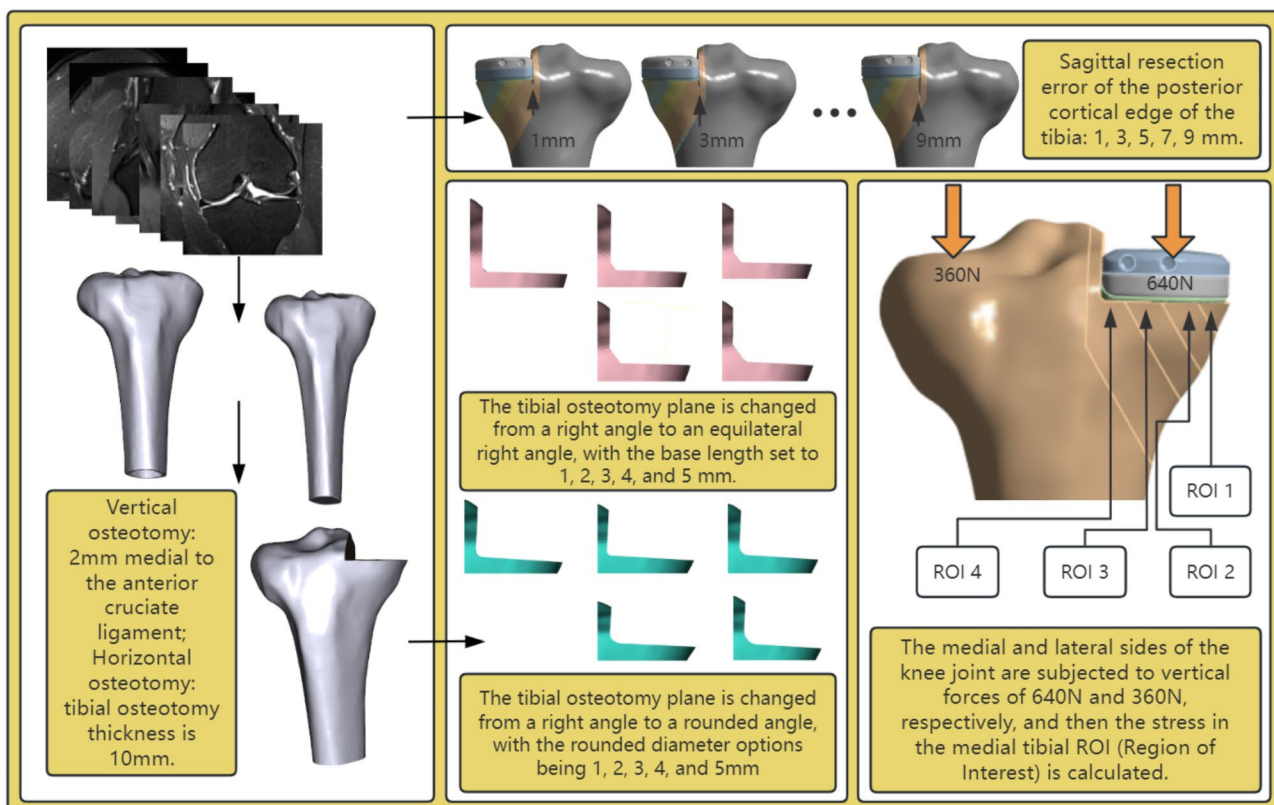


Fig. 1 Complete Finite Element Analysis Process, including image data collection, model modification, model construction, and mechanical analysis

the prosthesis was compared with the failure load reported by Clarius et al. [20, 21](Clarius et al., 2010). Method 3: The stress in the cancellous bone beneath the tibial prosthesis was compared with previous studies [15].

Results

Finite element model validation

Based on previous classic studies, the tibia was loaded using the same loading conditions described, and a high ROF region was observed in ROI 4. Under the maximum fracture load, ROI 4 formed a high-risk fracture line extending into the tibial cortex (Fig. 2), which matched the fracture path observed clinically, confirming the validity of the model. The average failure load reported by Clarius et al. for the tibia with normal standard osteotomy was 3.9 KN [21]. Under this loading condition, the maximum ROF value was 5.2, and the failure element volume was 128 mm³. When these values were exceeded, the fracture risk significantly increased. The corresponding maximum ROF value beneath the tibial prosthesis in our finite element model was 5.3, with a failure element volume of 132 mm³, which is close to the values reported in previous studies, demonstrating the model’s applicability. When comparing the stress values beneath the tibial prosthesis, in a study by Ma, under a 1000 N loading

condition, the stress on the upper surface of the cancellous bone beneath the prosthesis was approximately 0.5-1 MPa, which is similar to the stress values of 0.6–1.1 MPa obtained in our model, confirming the model’s usability [15].

Variation of equivalent stress in different rois under the tibial prosthesis

To study the variation of equivalent stress in different ROIs, models with vertical cutting errors of 1 mm, 3 mm, 5 mm, 7 mm, and 9 mm were analyzed. For ROI 1–3, the significance was greater than 0.05. However, for ROI 4, the results are shown in the table (Table 2). For further comparison, the equivalent stress of the first 20 nodes in ROI 4 was analyzed. It increased from 6.83 MPa to 10.55 MPa, showing a gradual increase. The maximum stress occurred at the vertical cutting edge. Analysis of the change pattern reveals that the equivalent stress increased significantly when the vertical cutting error changed from 5 mm to 7 mm, while the change was not significant from 1 mm to 5 mm (Fig. 3).

For the chamfer design models with 1 mm, 2 mm, 3 mm, 4 mm, and 5 mm, no significant differences were observed in ROI 1–4 across all nodes. However, when selecting nodes from the commonly fractured region in ROI 4, the equivalent stress of 20 randomly selected

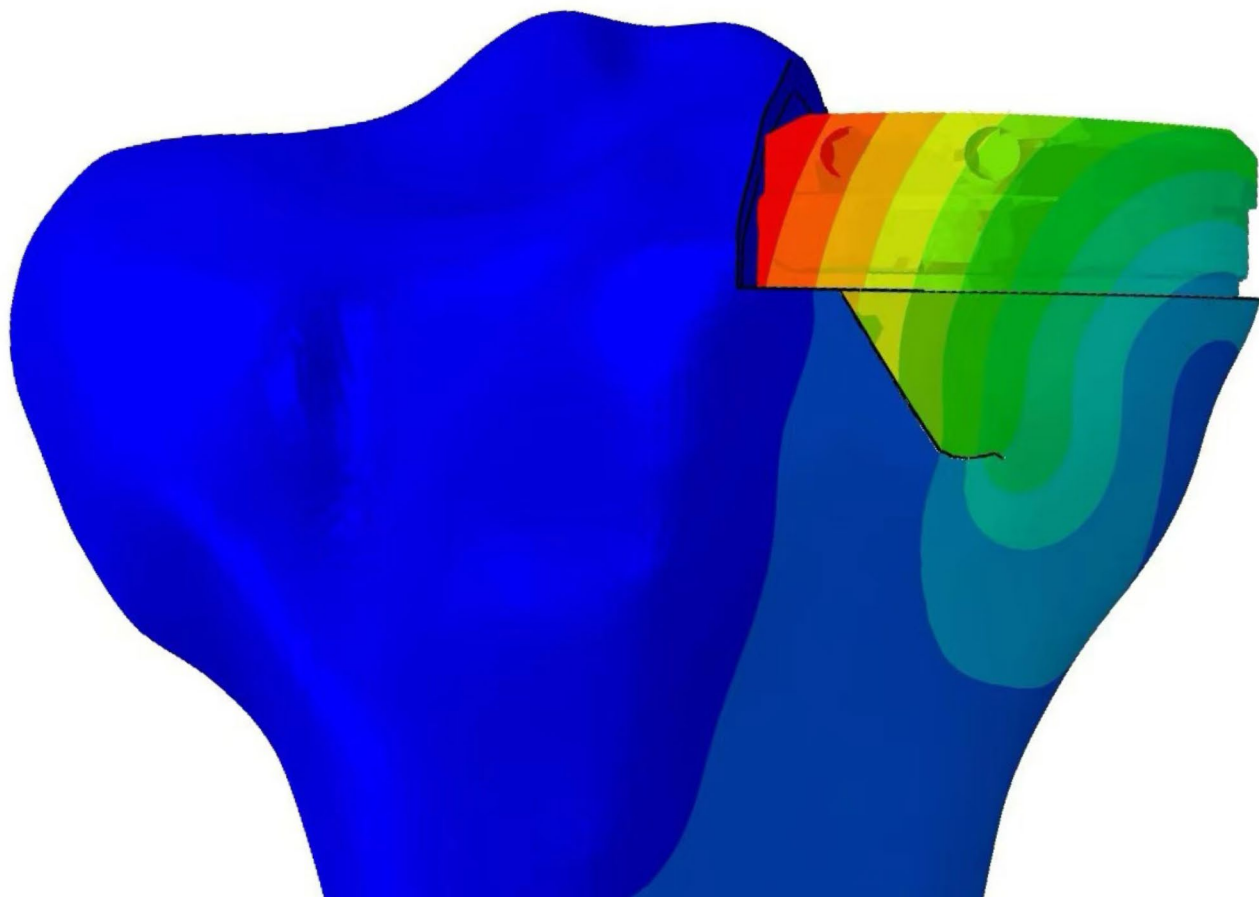


Fig. 2 Typical Fracture Model under Tibial Prosthesis

Table 2 In ROI 4, models with vertical cutting errors of 1 mm, 3 mm, 5 mm, 7 mm, and 9 mm were analyzed, and the results are shown in the table

	N	Mean	SD	t	p
Original	1678	3.2	1.43		
R014-1	4700	3.33	1.44	-3.267	0.001
R014-3	4674	3.34	1.47	-3.38	0.001
R014-5	4615	3.33	1.49	-3.196	0.001
R014-7	4591	3.36	1.54	-3.852	0
R014-9	4754	3.38	1.59	-4.435	0

nodes at the same location was further compared. The equivalent stress decreased from 5.65 MPa to 5.58 MPa, showing a gradual reduction. Analysis of the change pattern indicates that the equivalent stress values decrease as the chamfer size increases (Fig. 4). For the fillet design models with 1 mm, 2 mm, 3 mm, 4 mm, and 5 mm, no significant differences were observed in ROI 1–4 across all nodes. However, when selecting nodes from the commonly fractured region in ROI 4, the equivalent stress of 20 randomly selected nodes at the same location was further compared. The equivalent stress decreased from 5.65 MPa to 5.62 MPa, showing a gradual reduction.

Analysis of the change pattern indicates that the equivalent stress values decrease as the fillet size increases (Fig. 5).

Maximum principal strain / Elastic limit strain ratio in ROI

For the study of the ROF values of different ROIs, considering that the common fracture site is ROI 4, and no significant abnormalities were observed in ROIs 1–3 when calculating the equivalent stress values of different ROIs, the ROF values for ROI 1–3 were not further compared. For models with vertical cutting errors of 1, 3, 5, 7, and 9 mm, when selecting nodes from the common fracture region in ROI 4, we further compared the ROF of 20 randomly selected nodes at the same locations. These were compared with the original model, and the results are shown in the figure. The highest ROF is located at the vertical cutting site and distributes towards the distal tibia. (Fig. 6). For the models with chamfer designs of 1, 2, 3, 4, and 5 mm, as well as the models with fillet designs of 1, 2, 3, 4, and 5 mm, the 20 maximum principal strain values in the ROI 4 area were taken, and their ROF values were calculated. These were compared with the original model. The maximum principal strain values gradually

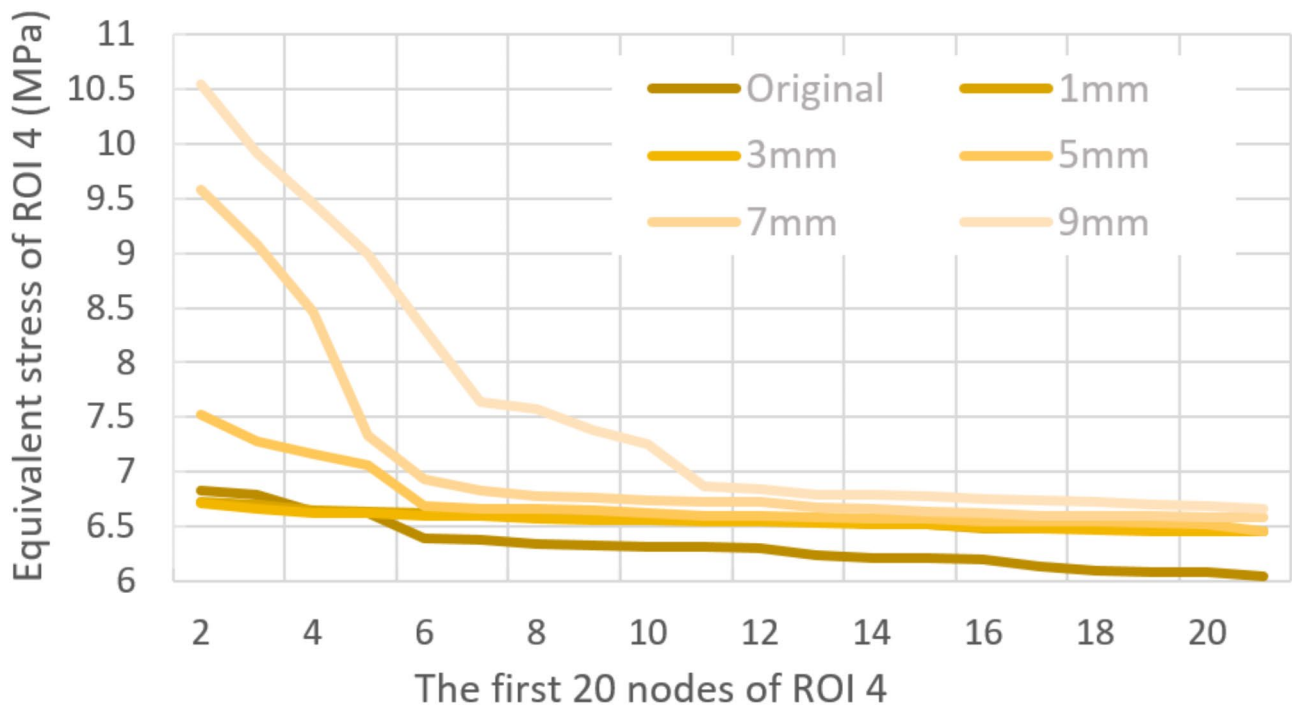


Fig. 3 Variation Trend of Equivalent Stress in the ROI 4 Area for the First 20 Nodes in Models with Different Vertical Cutting Errors

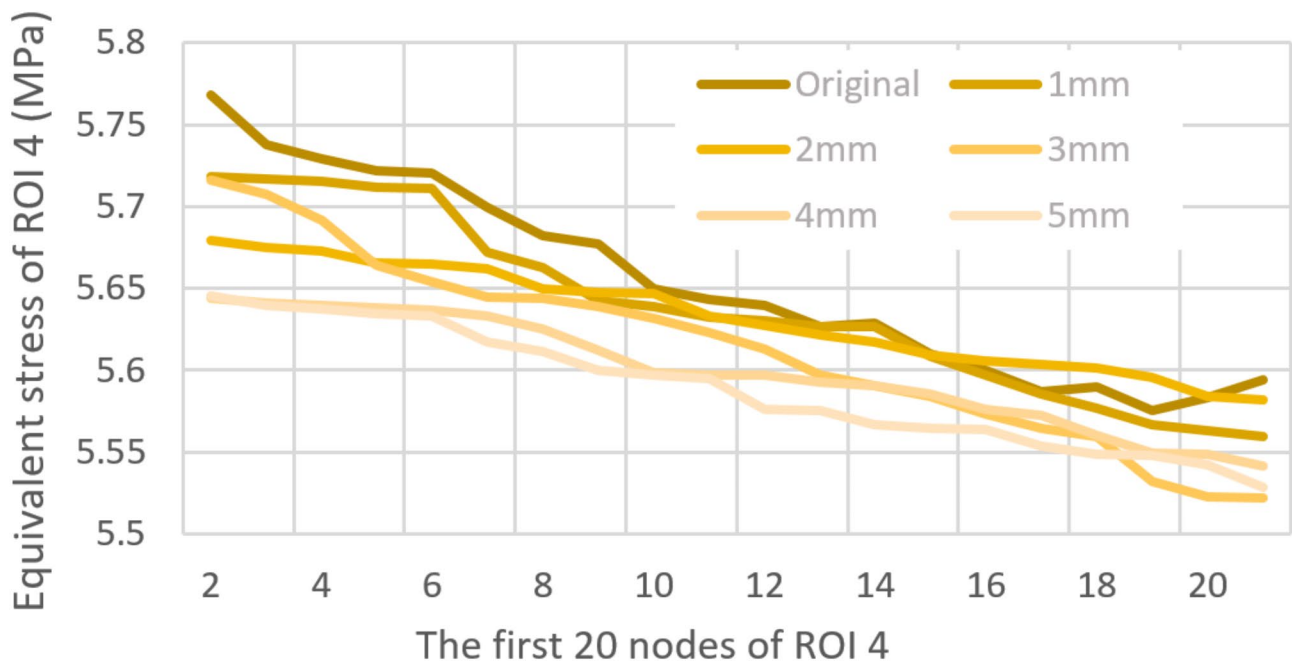


Fig. 4 Variation Trend of Equivalent Stress in the ROI 4 Area for the First 20 Nodes in Models with Different Chamfer Designs

decreased, and the ROF values followed a similar downward trend. Furthermore, as the diameter of the modified cutting surface increased, the rate of decrease slowed down. The results are shown in the figure. (Figures 7 and 8).

Discussion

The excellent clinical outcomes of unicompartamental knee arthroplasty (UKA) have been widely recognized by orthopedic surgeons and patients [1, 2, 22]. However, chronic pain and periprosthetic fractures caused by tibial degeneration after UKA have significant impacts. This study used finite element methods for knee joint

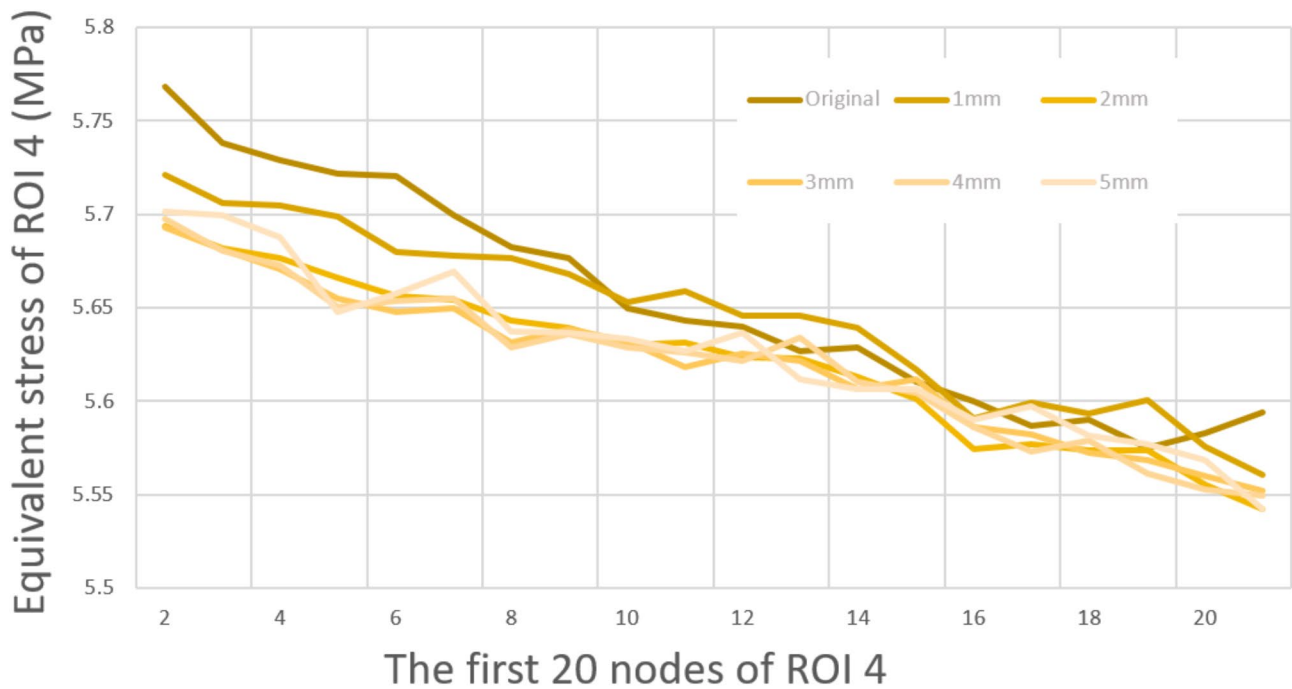


Fig. 5 Variation Trend of Equivalent Stress in the ROI 4 Area for the First 20 Nodes in Models with Different Fillet Designs

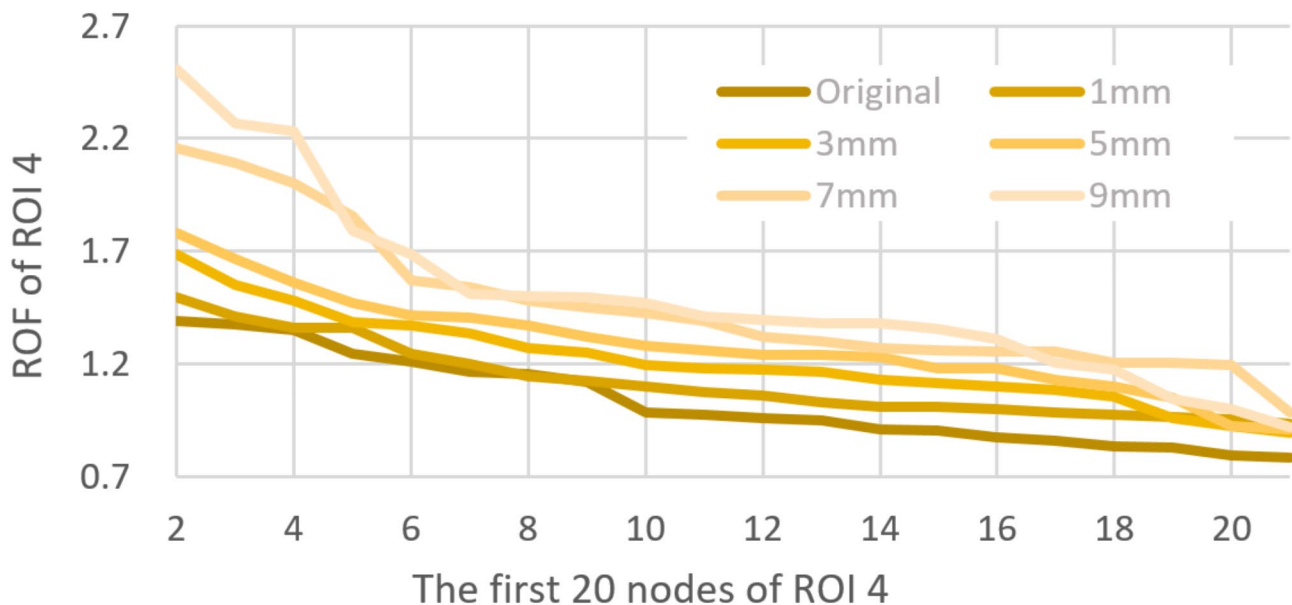


Fig. 6 Variation Trend of ROF in the ROI 4 Area for the First 20 Nodes in Models with Different Vertical Cutting Errors

modeling. After validating the model’s effectiveness, different vertical tibial cutting errors and surface modifications were simulated to assess their impact on UKA outcomes. The study concluded that tibial vertical cutting errors are high-risk factors for increasing fracture risk and accelerating bone degeneration. The larger the vertical cutting error, the higher the fracture risk and the faster the bone degeneration. When the tibial vertical cutting error exceeds 5 mm, the fracture risk beneath the

tibial prosthesis significantly increases. However, modifications to the vertical and horizontal cutting surfaces can reduce these risks.

All UKA procedures require the creation of an L-shaped space for the tibial component, which necessitates both horizontal resection and vertical cuts by the orthopedic surgeon. The tibial osteotomy module is a crucial component for creating this L-shaped space. This module is fixed to the front of the tibia and provides

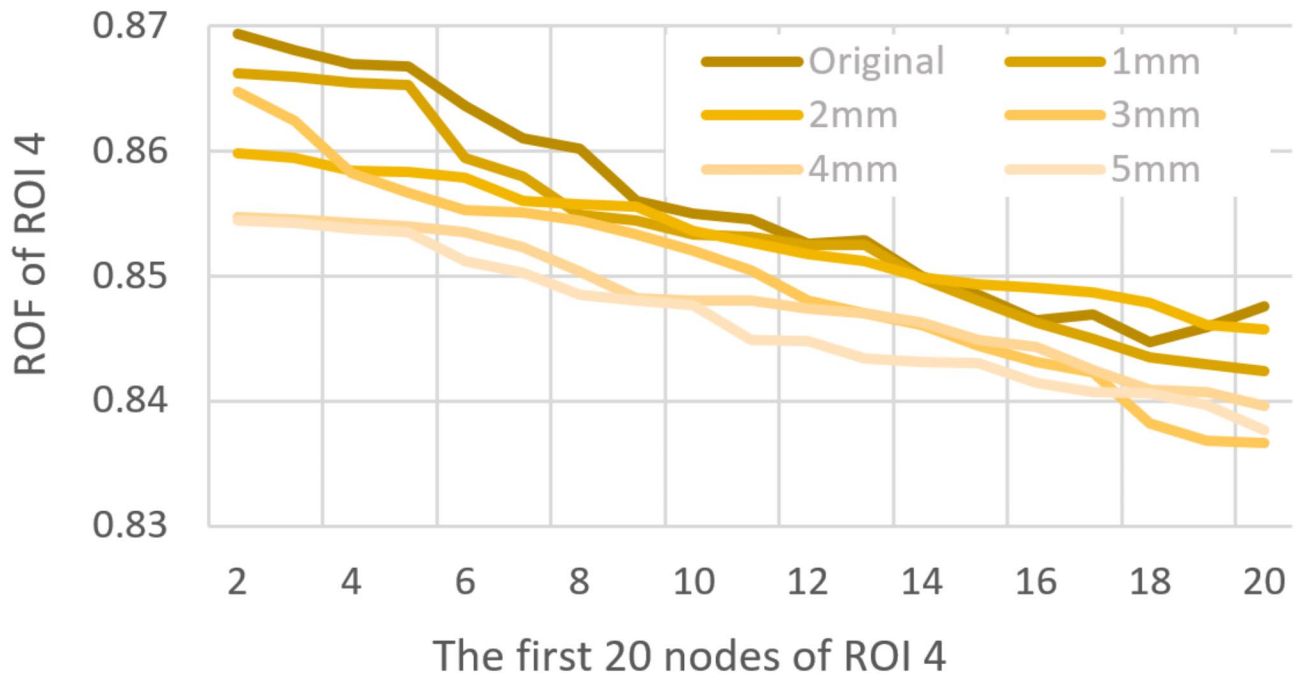


Fig. 7 Variation Trend of ROF in the ROI 4 Area for the First 20 Nodes in Models with Different Chamfer Designs

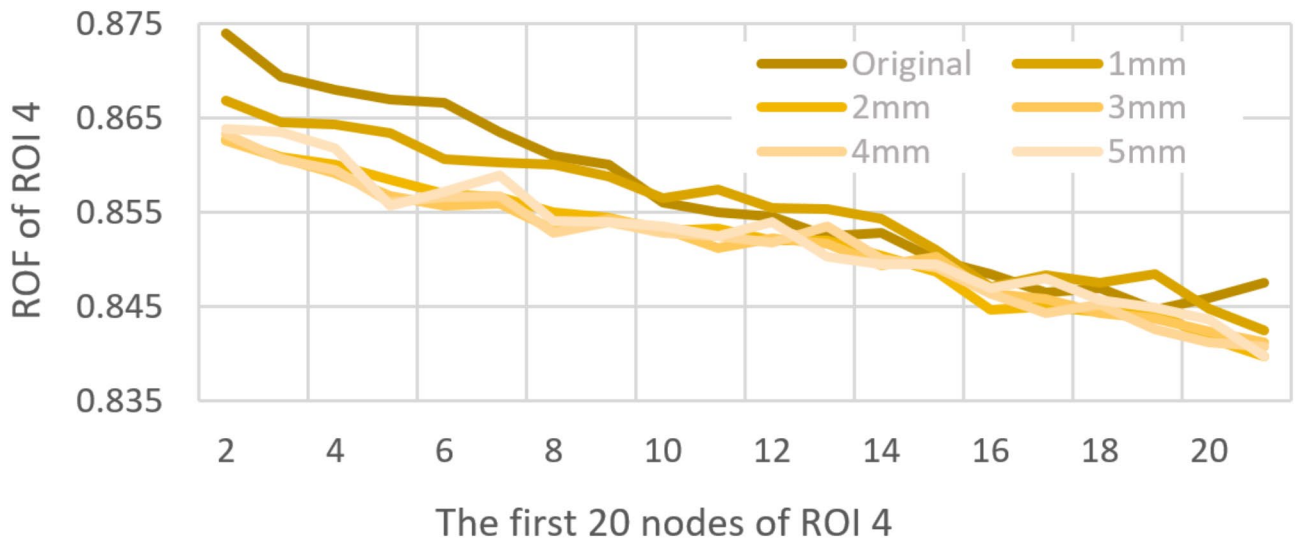


Fig. 8 Variation Trend of ROF in the ROI 4 Area for the First 20 Nodes in Models with Different Fillet Designs

accurate guidance for horizontal cuts while also limiting the vertical cut. However, it does not provide restriction at the posterior region during vertical cutting. In UKA, orthopedic surgeons need to perform osteotomy. Limited posterior visibility makes it difficult to identify the depth of the cut during surgery, often leading to vertical cutting errors, which is the focus of this study. In a study involving 100 bone specimens, 18% of the cases exhibited vertical cutting errors greater than 4.0 mm, and 3% of the cases had vertical cutting errors greater than 8.0 mm [10]. Therefore, we created different vertical cutting errors to study their impact on UKA.

Beneath the tibial prosthesis, the cortical bone bears most of the load transmitted by the tibial tray relative to the cancellous bone, as its elastic modulus is much higher than that of cancellous bone [23]. The abnormally high equivalent stress and strain in the medial proximal cortical bone beneath the tibial prosthesis are important causes of persistent pain after UKA [24]. When loading the UKA models with different vertical cutting errors, a noticeable increase in equivalent stress and strain beneath the tibial prosthesis was observed as the cutting error increased. A significant rise in equivalent strain was seen in ROI 4, with the highest equivalent strain in the

medial proximal cortical bone beneath the tibial prosthesis reaching 26,070 $\mu\epsilon$, which occurred in the 9 mm cutting error model. This is an extreme equivalent strain value. In our study, the compressive equivalent strain values in ROI 4 of the normal knee joint model were mostly in the range of 1500–4500 $\mu\epsilon$. However, for the vertical cutting error models, the compressive equivalent strain values in ROI 4 were significantly higher, and the ROF also showed a marked increase. Our findings are consistent with Clarius' research, which indicated that extended sagittal cuts in the tibia (greater than 8 mm) lead to a notch effect. The increased notch tension peaks weaken the bone's load-bearing capacity and result in fractures beneath the medial prosthesis. Furthermore, in their study, 18% of the cases with vertical cutting errors greater than 4.0 mm occurred with inexperienced surgeons [10, 21]. According to previous studies, a critical damage strain threshold of tensile equivalent strain greater than 2500 $\mu\epsilon$ and compressive equivalent strain greater than 4000 $\mu\epsilon$ may reduce bone remodeling capacity, leading to bone degeneration. On the other hand, stress shielding effects, where bone strain falls below 100 $\mu\epsilon$, can induce disuse mode remodeling and result in bone loss [25, 26].

This study did not consider osteoporosis as a factor. However, if unicompartmental knee arthroplasty is performed on patients with osteoporosis, it is likely to be accompanied by higher equivalent strains and an increased risk of fractures [27]. High equivalent strain at the bone-metal interface is considered one of the main factors leading to screw loosening and failure. Lewis' finite element model shows that when the equivalent strain in the region surrounding the metal exceeds 4000 $\mu\epsilon$, it significantly increases the risk of loosening and pain [28]. Abnormal strain values have become one of the causes of postoperative pain. As the vertical cutting error increases, there is a significant rise in equivalent stress and strain at the cut surface, with the highest values occurring at the deepest part of the cut. This not only leads to pain but also increases the risk of fractures. In the study by Pegg et al., the fracture risk standard proposed by Chileo et al. was referenced. This standard calculates the ROF value based on the ratio of maximum principal strain to elastic limit strain. The ROF threshold is 1, indicating that the strain has reached the elastic limit. When stress exceeds this threshold, local tissue may enter the plastic deformation region. When the ROF value exceeds 1, it indicates that the stress/strain in the local region has exceeded the bone's load-bearing capacity, and the fracture risk begins to increase. Additionally, it was pointed out that when the ROF value reaches 5, the local stress in the tibia significantly increases, indicating that the bone is under a higher risk of failure. Areas with stress exceeding this value show clear stress concentration, which may lead to localized fractures [20, 29].

The flawless execution of surgical techniques on patients has always been both a challenge and an achievement. The precision and complexity of the surgery place high technical demands on the surgeon, especially during the bone cutting process, where precise control over the vertical and horizontal cutting angles and depths is required [30].

A study by Chang suggested that compared to sharp right-angle orthogonal geometries, the radial angle features on the resection surface play a role in reducing strain and preventing bone degeneration. Their designed radial angle models can avoid extended bone cuts and reduce stress [24]. In our study, whether using chamfering or filleting designs, as the diameter of the chamfer or fillet increased, the equivalent stress decreased compared to the vertical osteotomy model, and consequently, the fracture risk also decreased. In a study by Clarius on how slight varus placement of the tibial component affects the keel-cortex distance and the incidence of tibial plateau fractures, the tibia was cut perpendicular to the tibial axis and compared with slight varus alignment using a new osteotomy guide. Postoperative 3D CT scans assessed the pre- and postoperative keel-cortex distance and the origin of the fracture line. The study ultimately concluded that a longer keel-cortex distance and slight varus alignment of the tibial component reduced the risk of postoperative tibial fractures [3]. There are many other studies focusing on ways to reduce the risk of periprosthetic fractures after UKA. In research comparing cemented and uncemented UKA, Hiranaka's study suggested that if preoperative X-rays indicate the need for a very small prosthesis or if the condyle is excessively prominent, cemented tibial fixation should be used [31]. A study by Seeger, which is similar to the aforementioned research, concluded that the load-bearing capacity of the tibial component in uncemented prostheses is significantly reduced. For patients with extended sagittal bone cuts, particularly those with poor bone quality, UKA carries a higher risk of periprosthetic tibial fractures [32].

However, this study also has certain limitations. First, the impact of osteoporosis on postoperative outcomes of UKA was not considered. Osteoporosis is common among patients and may exacerbate the risk of fractures and alter the biomechanical results, thereby affecting the generalizability of the study [33, 34]. Additionally, the finite element model used in this study was based on the tibial geometry of a 26-year-old male volunteer, which may not represent patients of different ages, body types, or health conditions. As such, the generalizability of the results is limited. Furthermore, the study primarily focused on vertical cutting errors and surface modification designs but did not consider other important factors that could affect postoperative outcomes, such as

the patient's activity level, muscle strength, and the use of surgical navigation technologies [35, 36].

Moreover, although the study used finite element analysis for simulations, it lacks clinical validation, and the simulation results may differ from actual surgeries due to the absence of clinical data support. Finally, the study did not explore in depth how variations in bone quality across different regions of the tibia affect stress and strain distribution, which could influence fracture risk and postoperative outcomes. Therefore, while this study holds certain theoretical value, a comprehensive understanding of the effects of vertical cutting errors and surface modifications on UKA still requires clinical validation and consideration of additional influencing factors [37, 38].

Conclusion

This study investigated the biomechanical effects of tibial vertical cutting errors on the proximal tibia after UKA and explored the use of surface modification designs to reduce fracture risk. The results showed that as cutting errors increased, the stress and fracture risk beneath the tibial prosthesis significantly increased, particularly when the cutting error exceeded 5 mm, at which point the fracture risk increased sharply. The modified cutting surface designs effectively reduced stress concentration and lowered postoperative fracture risk. Although the findings provide valuable insights into the impact of cutting errors on postoperative complications of UKA, some limitations remain. Future research should further explore the effects of other factors, such as osteoporosis, activity level, and muscle strength, on UKA outcomes and validate the results with clinical data.

Abbreviations

UKA	Unicompartmental knee arthroplasty
FEA	Finite element analysis
ROF	Risk of fracture
ROIs	Regions of interest
PE	Polyethylene

Acknowledgements

The completion of this study would not have been possible without the strong support and assistance of many individuals. I would like to express my heartfelt gratitude to the following individuals: First and foremost, I would like to sincerely thank Professor PSX for establishing the direction of the research and providing careful guidance throughout the entire study. I am grateful to DGY for their diligent and meticulous work ethic, which enabled the smooth progress of the research. My appreciation also goes to QGS, YYQ, PJW, HY, KHS, TSL and MYX for completing their respective tasks according to their assigned roles and providing valuable suggestions that contributed to the successful completion of the study.

Author contributions

ODY and PSX propose ideas, collect data, analyze data, write articles, and review articles. DGY, QGS, HY, MYX and TSL collect and analyze data. KHS, PJW and DGY collect data, analyze data, and make graphs. YYQ, PSX, KHS, analyze data and write articles. ODY, KHS and TSL prepare the manuscript. ODY, PSX, KHS, PJW review articles and modify articles.

Funding

This study did not receive any funding or financial support.

Data availability

The datasets used and/or analysed during the current study are available from the corresponding author on reasonable request. We are happy to provide the original data upon request.

Declarations

Ethics approval and consent to participate

Before the study, we called the members of the Ethics Committee for discussion, which was finally approved by the Ethics Committee of Wuzhou Red Cross Hospital and agreed to carry out the study. At the same time, we also communicated with the patient and his relatives about his condition and got their consent. This study was approved by the hospital ethics committee and carried out in accordance with the principles of the 1964 Helsinki Declaration revised in 2013. All the collected clinical data and imaging data were known to the patients and obtained the informed consent of the patients themselves.

Consent for publication

The volunteer agree to publication and sign written consent.

Competing interests

The authors declare no competing interests.

Author details

¹Department of Limb and Joint Ward, Wuzhou Red Cross Hospital, Wuzhou, Guangxi Province, China

²Department of Spine Ward, Affiliated Hospital of Guilin Medical College, Guilin, Guangxi Province, China

³Department of Brest Surgery Department, Wuzhou Red Cross Hospital, Wuzhou, Guangxi Province, China

⁴Department of Medical Imaging Department, Wuzhou Red Cross Hospital, Wuzhou, Guangxi Province, China

⁵Department of Spine Ward, Wuzhou Red Cross Hospital, Wuzhou, Guangxi Province, China

Received: 5 January 2025 / Accepted: 7 April 2025

Published online: 09 May 2025

References

1. Murray DW, Parkinson RW. Usage of unicompartmental knee arthroplasty. *Bone Joint J.* 2018;100-B:432–5.
2. Crawford DA, Berend KR, Thienpont E. Unicompartmental knee arthroplasty: US and global perspectives. *Orthop Clin North Am.* 2020;51:147–59.
3. Pandit H, et al. Medial tibial plateau fracture and the Oxford unicompartmental knee. *Orthopedics.* 2007;30:28–31.
4. Kumar A, Chambers I, Wong P. Periprosthetic fracture of the proximal tibia after lateral unicompartmental knee arthroplasty. *J Arthroplasty.* 2008;23:615–8.
5. Rudol G, Jackson MP, James SE. Medial tibial plateau fracture complicating unicompartmental knee arthroplasty. *J Arthroplasty.* 2007;22:148–50.
6. Berger RA, et al. Results of unicompartmental knee arthroplasty at a minimum of ten years of follow-up. *J Bone Joint Surg Am.* 2005;87:999–1006.
7. NJR. NJR Annual Report 2022 - The National Joint Registry. <https://www.njrce.ntrc.org.uk/njr-annual-report-2022/> (2022).
8. Douiri A, et al. Functional scores and prosthetic implant placement are different for navigated medial UKA left in varus alignment. *Knee Surg Sports Traumatol Arthrosc.* 2023;31:3919–26.
9. Zhu G-D, Guo W-S, Zhang Q-D, Liu Z-H, Cheng L-M. Finite element analysis of Mobile-bearing unicompartmental knee arthroplasty: the influence of tibial component coronal alignment. *Chin Med J (Engl).* 2015;128:2873–8.
10. Clarius M, Aldinger PR, Bruckner T, Seeger JB. Saw cuts in unicompartmental knee arthroplasty: an analysis of sawbone preparations. *Knee.* 2009;16:314–6.
11. Houskamp DJ, Tompane T, Barlow BT. What is the critical tibial resection depth during unicompartmental knee arthroplasty?? A Biomechanical study of fracture risk. *J Arthroplasty.* 2020;35:2244–8.

12. Stoddart JC, Garner A, Tuncer M, Cobb JP, van Arkel RJ. The risk of tibial eminence avulsion fracture with bi-unicondylar knee arthroplasty: a finite element analysis. *Bone Joint Res.* 2022;11:575–84.
13. Dai X, et al. How does the inclination of the tibial component matter? A three-dimensional finite element analysis of medial mobile-bearing unicompartmental arthroplasty. *Knee.* 2018;25:434–44.
14. Dao Trong ML, Diezi C, Goerres G, Helmy N. Improved positioning of the tibial component in unicompartmental knee arthroplasty with patient-specific cutting blocks. *Knee Surg Sports Traumatol Arthrosc.* 2015;23:1993–8.
15. Ma P, et al. Biomechanical effects of fixed-bearing femoral prostheses with different coronal positions in medial unicompartmental knee arthroplasty. *J Orthop Surg Res.* 2022;17:150.
16. Shirram D, Praveen Kumar G, Cui F, Lee YHD, Subburaj K. Evaluating the effects of material properties of artificial meniscal implant in the human knee joint using finite element analysis. *Sci Rep.* 2017;7:6011.
17. Nie Y, Yu Q, Shen B. Impact of tibial component coronal alignment on knee joint biomechanics following Fixed-bearing unicompartmental knee arthroplasty: A finite element analysis. *Orthop Surg.* 2021;13:1423–9.
18. Du M, et al. Tibio-Femoral contact force distribution of knee before and after total knee arthroplasty: combined finite element and gait analysis. *Orthop Surg.* 2022;14:1836–45.
19. ISO 14242-3. Implants for surgery-wear of total hip-joint prostheses-Part 3: loading and displacement parameters for orbital bearing type wear testing machines and corresponding environmental conditions for test. 2014.
20. Pegg EC, et al. Minimising tibial fracture after unicompartmental knee replacement: A probabilistic finite element study. *Clin Biomech (Bristol Avon).* 2020;73:46–54.
21. Clarius M, et al. Periprosthetic tibial fractures in unicompartmental knee arthroplasty as a function of extended sagittal saw cuts: an experimental study. *Knee.* 2010;17:57–60.
22. Argenson JN, Beaufils P. Unicompartmental knee arthroplasty: is a reappraisal in order? *Orthop Traumatol Surg Res.* 2018;104:941–2.
23. Carter DR, Hayes WC. The compressive behavior of bone as a two-phase porous structure. *J Bone Joint Surg Am.* 1977;59:954–62.
24. Chang T-W, et al. Biomechanical evaluation of proximal tibial behavior following unicondylar knee arthroplasty: modified resected surface with corresponding surgical technique. *Med Eng Phys.* 2011;33:1175–82.
25. Frost HM. A 2003 update of bone physiology and Wolff's law for clinicians. *Angle Orthod.* 2004;74:3–15.
26. Pattin CA, Caler WE, Carter DR. Cyclic mechanical property degradation during fatigue loading of cortical bone. *J Biomech.* 1996;29:69–79.
27. Crawford RP, Cann CE, Keaveny TM. Finite element models predict in vitro vertebral body compressive strength better than quantitative computed tomography. *Bone.* 2003;33:744–50.
28. Lewis GS, Mischler D, Wee H, Reid JS, Varga P. Finite element analysis of fracture fixation. *Curr Osteoporos Rep.* 2021;19:403–16.
29. Schileo E, Taddei F, Cristofolini L, Viceconti M. Subject-specific finite element models implementing a maximum principal strain criterion are able to estimate failure risk and fracture location on human femurs tested in vitro. *J Biomech.* 2008;41:356–67.
30. Zhang Q-D, et al. A modified technique for tibial bone sparing in unicompartmental knee arthroplasty. *Chin Med J (Engl).* 2019;132:2690–7.
31. Hiranaka T, et al. Tibial shape and size predicts the risk of tibial plateau fracture after cementless unicompartmental knee arthroplasty in Japanese patients. *Bone Joint J.* 2020;102-B:861–7.
32. Seeger JB, et al. Extended sagittal saw cut significantly reduces fracture load in cementless unicompartmental knee arthroplasty compared to cemented tibia plateaus: an experimental cadaver study. *Knee Surg Sports Traumatol Arthrosc.* 2012;20:1087–91.
33. Zhuang Z, et al. Prevalence of osteoporosis in patients awaiting unicompartmental knee arthroplasty: a cross-sectional study. *Front Endocrinol (Lausanne).* 2023;14:1224890.
34. Liu M, Jiang K, Ju X. Biomechanical effects of femoral prosthesis misalignment on the structure of the lateral compartment during medial unicompartmental knee arthroplasty in osteoporotic patients. *J Orthop Surg (Hong Kong).* 2024;32:10225536241273924.
35. Catani F, et al. Muscle activity around the knee and gait performance in unicompartmental knee arthroplasty patients: a comparative study on fixed- and mobile-bearing designs. *Knee Surg Sports Traumatol Arthrosc.* 2012;20:1042–8.
36. Heyse TJ, et al. UKA closely preserves natural knee kinematics in vitro. *Knee Surg Sports Traumatol Arthrosc.* 2014;22:1902–10.
37. Batailler C, et al. Improved sizing with image-based robotic-assisted system compared to image-free and conventional techniques in medial unicompartmental knee arthroplasty. *Bone Joint J.* 2021;103-B:610–8.
38. Banger MS, et al. Are there functional Biomechanical differences in robotic arm-assisted bi-unicompartmental knee arthroplasty compared with conventional total knee arthroplasty? A prospective, randomized controlled trial. *Bone Joint J.* 2022;104-B:433–43.

Publisher's note

Springer Nature remains neutral with regard to jurisdictional claims in published maps and institutional affiliations.